

## Neutron/gamma discrimination employing the power spectrum analysis of the signal from the liquid scintillator BC501A

X.L. Luo\*, Y.K. Wang, J. Yang, G. Liu, C.B. Lin, Q.Q. Hu, J.X. Peng

Department of Instrument Science and Technology, College of Mechatronics and Automation, National University of Defense Technology, Changsha, China

### ARTICLE INFO

#### Article history:

Received 24 August 2012

Received in revised form

2 April 2013

Accepted 2 April 2013

Available online 10 April 2013

#### Keywords:

$n/\gamma$  discrimination

Power spectrum

Liquid scintillator

Reference-pulses

### ABSTRACT

A digital method for the discrimination of neutron and  $\gamma$ -ray events based on analyzing the power spectra of the signals from a BC501A liquid scintillator detector was presented and investigated in this paper. In order to evaluate the feasibility of this novel pulse shape discrimination method, a 5GSample/s 8-bit oscilloscope was used to acquire waveforms for  $n/\gamma$  discrimination. Furthermore, the performance of this novel  $n/\gamma$  discrimination method was compared with that of a widely used method called *the reference-pulses method* which averaged a large number of neutron and  $\gamma$ -ray pulses to obtain the reference-pulse as the criterion for  $n/\gamma$  discrimination. The results showed that the proposed method performed well over *the reference-pulses method*, which was verified by the considerable decrease in the error rate of  $n/\gamma$  discrimination and the improvement of the Figure of Merit.

© 2013 Elsevier B.V. All rights reserved.

### 1. Introduction

Liquid scintillators are widely used in fast neutron detection because of their excellent pulse shape discrimination (PSD) properties and fast timing performance. In most cases the accurate discrimination between neutrons and  $\gamma$  rays is essential since liquid scintillators are sensitive to both neutrons and  $\gamma$ -ray photons [1]. Over the past few decades many PSD techniques for  $n/\gamma$  discrimination, which are based on the principle that the decay rate of the light output of a liquid scintillator depends on the radiation types, have been developed and studied. The traditional methods of  $n/\gamma$  discrimination, including the rise-time method [2,3] and the charge-comparison method [4,5], exploit analog techniques which require dedicated analog electronic modules with complex circuits and poor stability. The rise-time method implies the determination of the time at which the integrated light output reaches a certain fraction of its maximum, while the charge-comparison method implies essentially the determination of the relative weight of the amounts of light emitted respectively in the fast and slow component of the light pulse. The implementation of the charge-comparison method generally relies upon the integration of the pulse over two different intervals, whose choice depends on the actual experimental set-up adopted. The statistics of this method is much simpler than that of the rise-time technique, being essentially driven by the binomial law. In general,

the charge-comparison approach performs better than the rise-time method [6].

More recently, there has been a turning point in  $n/\gamma$  discrimination in accordance with the advent of related fast and high resolution digital devices such as A/D converters, digital signal processors (DSPs), and field programmable gate arrays (FPGAs). These digital processors can sample and store the complete waveform of the liquid scintillator signals for post-processing, thus have offered the feasibility to transport the traditional PSD algorithms into the digital framework and also opened a new window for the digital  $n/\gamma$  discrimination techniques that afford additional benefits in terms of speed and discrimination performance. For example, Moszynski et al. [7] carried out the study of the  $n/\gamma$  discrimination for a large volume BC501A liquid scintillator coupled to a 130 mm diameter XP4512B photomultiplier (PMT) by the digital charge-comparison method and achieved a very good  $n/\gamma$  discrimination down to 100 keV of recoil electron energy. Ambers et al. [8] presented a hybrid PSD method which combines a charge-comparison PSD method with a reference-pulses PSD method, and the results demonstrated that the method gave considerable improvement over the charge-comparison method for light output bins below 70 keVee. S. Marrone et al. [9] described an algorithm based on the fit of an analytical shape (three exponential functions) to the recorded signals, and the performance of this method, both in terms of energy resolution and particle identification, is comparable to that of the charge-comparison method. In addition, several original digital methods have recently been developed such as the correlation method [10], the method of pulse gradient analysis (PGA) [11–13], the method of artificial neural networks [14], the fuzzy  $c$ -means algorithm

\* Corresponding author. Tel.: +86 731 84573353; fax: +86 731 84574962.  
E-mail address: delongtmac@163.com (X.L. Luo).

[15], the wavelet algorithm [16,17], and the method of frequency gradient analysis (FGA) [18,19].

In summary, all of the above mentioned methods have been implemented successfully for  $n/\gamma$  discrimination in terms of some specific aspect of discrimination performance. However, most of them exploit directly the pulse response arising from the PMT, often by averaging a large number of neutron and  $\gamma$ -ray pulses to obtain the reference-pulse as the criterion for  $n/\gamma$  discrimination, i. e. *the reference-pulses method*. Since the signal response of the scintillant cell and the PMT is statistical and very noisy, the natural variance in the pulse shape may deteriorate the  $n/\gamma$  discrimination performance of these PSD methods. In this paper, we propose a new  $n/\gamma$  discrimination method which is based on analyzing the power spectrum of the detector signal. The primary consideration of this research is to decrease the sensitivity to pulse variation and improve the  $n/\gamma$  discrimination performance of the PSD method by transforming the signal into the frequency-domain. The method has been tested using the Time-of-Flight (TOF) measurement system described in Section 2. In Section 3, the principle of the method is given and its  $n/\gamma$  discrimination performance is investigated by comparing with that of *the reference-pulses PSD method*. Finally, the conclusions arising from this research are stated in Section 4.

## 2. The experiment

The experimental data analyzed in this work were acquired using the TOF measurement system at the Institute of Nuclear Physics and Chemistry, the Chinese Academy of Engineering Physics, Mianyang, China. As shown in Fig. 1, through deuterium–tritium fusion reaction, an associated particle neutron generator (APNG) produces neutrons and alpha particles that are correlated in time and travel in opposite directions to conserve momentum. The energies of neutrons and alpha particles are 14.1 MeV and 3.5 MeV, respectively.

For TOF research, one plastic scintillation detector detects the arrival of the alpha particle beam pulse and provides a timing reference point for the arrival of each pulse and is referred to as the beam-pickup signal, and the other liquid scintillation detector placed at an adjustable distance from the tritiated target detects the corresponding neutrons or  $\gamma$  rays. The plastic scintillation detector consisted of a  $\phi 25.4 \text{ mm} \times 0.1 \text{ mm}$  cylindrical cell scintillation detector, optically-coupled to an EMI 9807B PMT, which was operated with a negative supply voltage of  $-1600 \text{ V DC}$ .

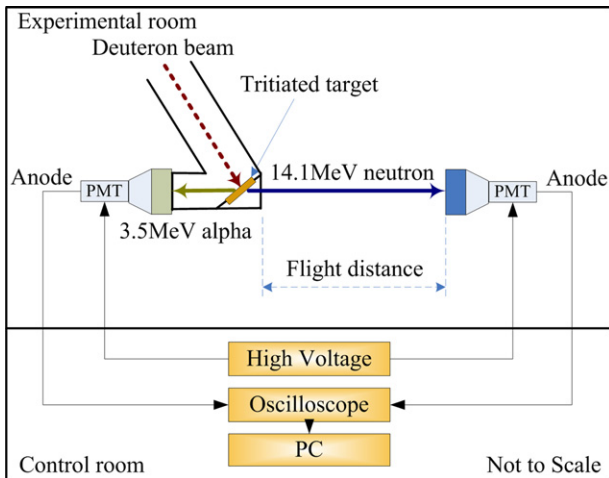


Fig. 1. A schematic of the experimental set-up used for the associated particle neutron generator at the Institute of Nuclear Physics and Chemistry, the Chinese Academy of Engineering Physics, Mianyang, China.

The output signal from the plastic scintillator was connected to Channel 1 of a Tektronic digital phosphor oscilloscope (DPO) 4104, via approximately 25 m of high bandwidth cable. The liquid scintillation detector consisted of a  $\phi 50.8 \text{ mm} \times 50.8 \text{ mm}$  cylindrical cell scintillation detector filled with BC501A organic liquid, optically-coupled to another EMI 9807B PMT, which was operated with a negative supply voltage of  $-1400 \text{ V DC}$ . The output signal from the liquid scintillator was connected to another input of the digital oscilloscope and used to trigger acquisition.

The liquid scintillator pulse and the corresponding beam-pickup pulse data were captured digitally with the Tektronix DPO4104 with 8-bit resolution working at 5GSample/s. This enabled all detected events, both  $\gamma$  rays and neutrons, to be sorted in terms of their time-of-arrival relative to the initial beam-pickup. Based on the difference in flight time for neutrons and  $\gamma$  rays across the known flight path length, we extracted 2304 neutron and 1103  $\gamma$ -ray pulses for the research on  $n/\gamma$  discrimination in this paper. The misidentification rate of the TOF method in this experiment for neutron and  $\gamma$ -ray pulses are approximately 0.012 and 0.008 respectively because of the scattered events and other accidental particles. Since TOF is in general a high-accuracy method of  $n/\gamma$  discrimination, the results of TOF can be used for the research of  $n/\gamma$  discrimination with the PSD methods in Section 3.

## 3. $n/\gamma$ discrimination with PSD methods

The pulse processing began with the removal of the baseline shift where a constant baseline shift was calculated in the pre-trigger range of the captured signal and then subtracted from the digitized waveform to retrieve its original pulse with zero-baseline drift. The starting time of each signal was defined as the time when it reaches 10% of its maximum amplitude and the duration of the pulse was set to 110 ns. These pulses were subsequently sorted out into three pulse height bins ranging from 0.25 to 8.30 MeVee, i.e. bin 1 (1714 pulses, 0.25–2.25 MeVee), bin 2 (820 pulses, 2.25–5.60 MeVee) and bin 3 (873 pulses, 5.60–8.30 MeVee).

### 3.1. The power spectrum PSD method

The concept of the power spectrum of a signal is fundamental in electrical engineering, especially in electronic communication systems, often being used to identify the frequency components of the signal. However, no research has been devoted to the application of the power spectrum in  $n/\gamma$  discrimination. Since the pulse shape of the neutron-induced signal is different from that of the  $\gamma$ -induced signal, in this section we will attempt to investigate the  $n/\gamma$  discrimination by observing and measuring the power spectrum of the output signals in the experiment.

For continuous signals that describe for example stochastic physical processes, the power spectrum gives a plot of the portion of a signal's power falling within given frequency bins. Here, power can be the actual physical power, or more often, for convenience with abstract signals, can be defined as the squared value of the signal. The power spectrum of a given signal  $x(t)$  is defined as

$$P(\omega) = \lim_{T \rightarrow \infty} \frac{1}{T} |X_T(\omega)|^2 \quad (1)$$

where  $\omega$  is the normalized discrete-time frequency and  $X_T(\omega)$  is the Fourier transform of the signal  $x(t)$  in period  $T$ , i.e.

$$X_T(\omega) = \int_0^T x(t) \exp(-j\omega t) dt \quad (2)$$

In this study, the neutron and  $\gamma$ -ray pulses with the pulse period of 110 ns were sampled with a digital phosphor oscilloscope working at 5GSample/s. Thus for each pulse acquired, a finite-length sequence  $x[n]$  of length  $N$  ( $N=550$ ) samples was actually recorded. According to the power spectrum estimation technique called periodogram [20], we firstly take the Fourier transform of the signal  $x[n]$

$$X(e^{j\omega}) = \sum_{n=0}^{N-1} x[n]e^{-j\omega n} \quad (3)$$

Then we can calculate the power spectrum of the signal  $x[n]$  as:

$$P(\omega) = \frac{1}{N} |X(e^{j\omega})|^2 \quad (4)$$

In this way we obtained the power spectra of a total of 2304 neutron and 1103  $\gamma$ -ray pulses. Fig. 2a shows the power spectra of individual neutron and  $\gamma$ -ray pulses in the frequency range from 0 to  $\pi$ . Subsequently, the reference neutron power spectra of three pulse height bins were computed by averaging the power spectra of neutron pulses in each bin respectively, and the reference gamma power spectrum was obtained in the same way which is shown in Fig. 2b. It can be observed from Fig. 2b that below the discrete-time frequency  $\pi/5$  the amplitude of the reference power spectra of neutron pulses in bin 1 and 2 are greater than that of  $\gamma$ -ray pulses while the reference neutron power spectrum for bin 3 is greater than the reference gamma power spectrum just below the discrete-time frequency  $3\pi/10$ . Furthermore, the reference neutron power spectra decreases more sharply than the reference gamma power spectrum in general. These distinct differences between the power spectra of neutron and  $\gamma$ -ray pulses make it feasible to accomplish n/ $\gamma$  discrimination based on analyzing the power spectrum of the signal.

For an “unknown” measured pulse in each bin, the power spectrum was calculated firstly and then compared point-by-point to the reference power spectra of neutron pulses of its bin and  $\gamma$ -ray pulses. The Chi Square ( $\chi^2$ ) [21] was employed to test the differences between the power spectrum of the measured pulse and the reference power spectrum of neutron and  $\gamma$ -ray pulses, i.e.

$$\chi_{n,P}^2 = \sum_i \frac{(\hat{P}_i - P_{n,i})^2}{P_{n,i}}, \quad \chi_{\gamma,P}^2 = \sum_i \frac{(\hat{P}_i - P_{\gamma,i})^2}{P_{\gamma,i}} \quad (5)$$

where  $\hat{P}_i$  is the  $i$ -th sample of the power spectrum of the measured pulse,  $P_{n,i}$  and  $P_{\gamma,i}$  are the  $i$ -th samples of the reference power spectrum of neutron and  $\gamma$ -ray pulses, respectively. Then the n/ $\gamma$  discrimination parameter is defined as

$$D_P = \chi_{\gamma,P}^2 - \chi_{n,P}^2 \quad (6)$$

Traditionally, the quality of an n/ $\gamma$  discrimination method is often assessed qualitatively by plotting the amplitude of a given pulse against a discrimination parameter [11–13,18,19,22]. In this study, with the plot of peak amplitude of each pulse versus the discrimination parameter  $D_P$  in Figs. 3–5a, two well-separated groups of events can be observed, each of which corresponding to neutron or  $\gamma$ -ray events. It is seen that each point in the plane has been tagged with the pulse type that TOF has assigned to it, which can provide an independent basis for the identification of radiation type alongside the *power spectrum PSD method*. Besides, the neutron and  $\gamma$ -ray plumes have been separated by using a discrimination line on each plot that represents the best separation boundary, which is an established technique [23] whereby the centroid of each cluster of data is identified and a linear fit is applied to the midpoints between the clusters. In Fig. 3a for instance, if  $D_P$  is positive, which means that the differences

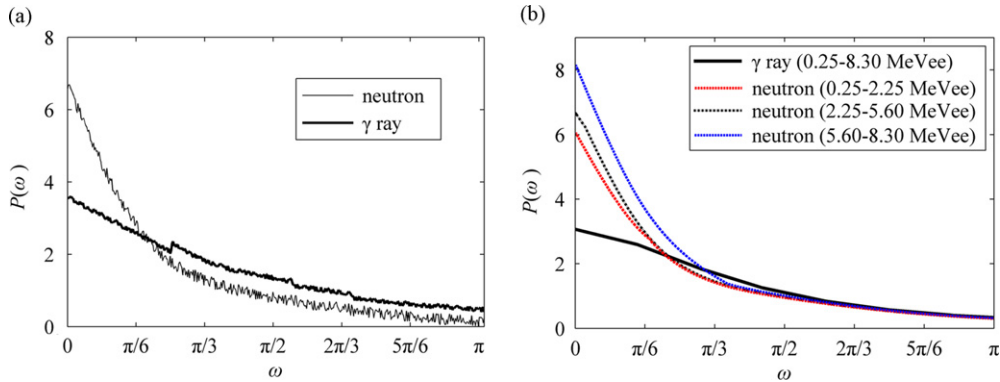


Fig. 2. (a) The power spectra of individual neutron and  $\gamma$ -ray pulses. (b) The reference power spectra of neutron and  $\gamma$ -ray pulses.

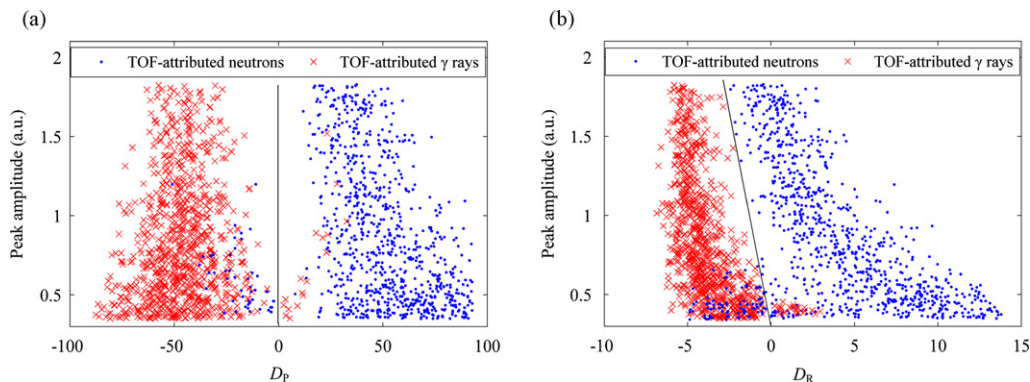
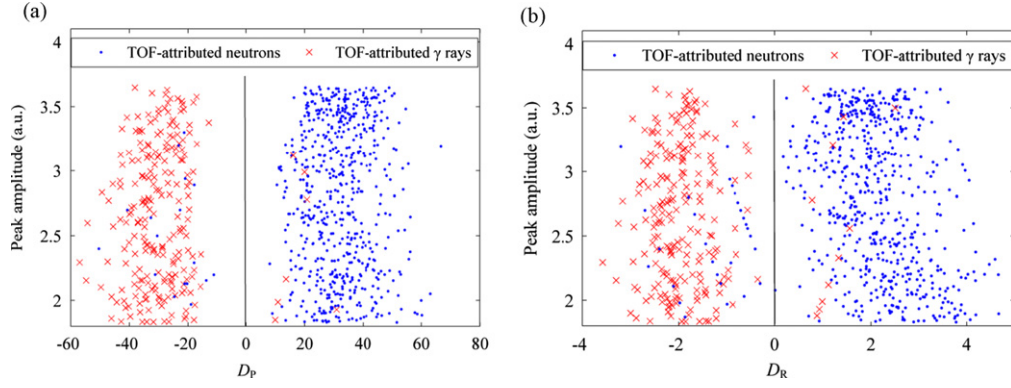
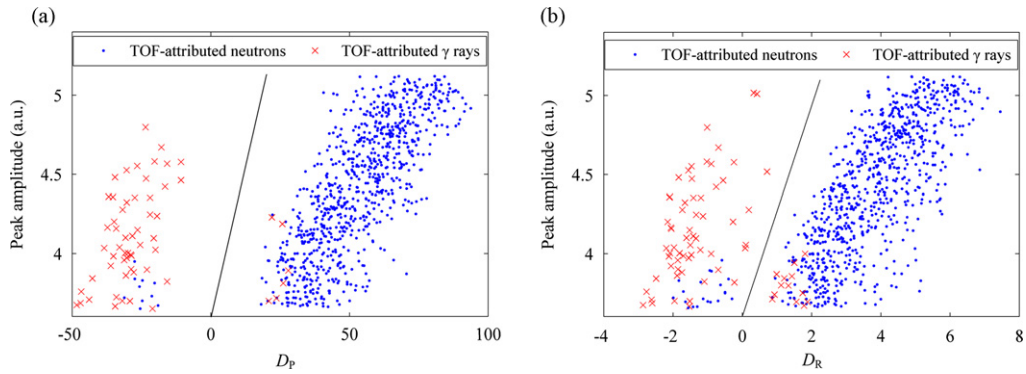


Fig. 3. Scatter plots of peak amplitude against the discrimination parameter of the PSD methods for 1714 pulses in bin 1 (0.25–2.25 MeVee). A line is included on each to indicate the threshold between neutrons and  $\gamma$  rays. (a) *The power spectrum PSD method*, and (b) *the reference-pulses method*.



**Fig. 4.** Scatter plots of peak amplitude against the discrimination parameter of the PSD methods for 820 pulses in bin 2 (2.25–5.60 MeVee). A line is included on each to indicate the threshold between neutrons and  $\gamma$  rays. (a) *The power spectrum PSD method*, and (b) *the reference-pulses method*.



**Fig. 5.** Scatter plots of peak amplitude against the discrimination parameter of the PSD methods for 873 pulses in bin 3 (5.60–8.30 MeVee). A line is included on each to indicate the threshold between neutrons and  $\gamma$  rays. (a) *The power spectrum PSD method*, and (b) *the reference-pulses method*.

between the power spectrum of the measured pulse and the reference power spectrum of neutron  $\gamma$ -ray pulses ( $\chi_{\gamma,p}^2$ ) is greater than the differences between the power spectrum of the measured pulse and the reference power spectrum of neutron pulses ( $\chi_{n,p}^2$ ), the measured pulse would be classified as a neutron event on basis of the *power spectrum PSD method*, whilst if negative the measured pulse can be identified as a  $\gamma$ -ray event. Therefore, the events located on the right side of the discrimination line are identified as neutrons and the left groups of events are regarded as  $\gamma$  rays in Fig. 3a according to the *power spectrum PSD method*. Most of the TOF-attributed neutrons and  $\gamma$  rays are located in the expected region of the scatter plot corresponding to their TOF assignments while there are some events being mistakenly classified by the *power spectrum PSD method*, which will be discussed in Section 3.

### 3.2. PSD with the reference-pulses method

In our research, we chose the *reference-pulses PSD method* [8,22,24] that has received wide acceptance as a reference to evaluate the n/ $\gamma$  discrimination performance of the *power spectrum PSD method*. The same 3407 pulses processed in Section 3.1 were applied to the *reference-pulses method*. First, these signals were normalized to maximum in order to remove the dependency of the *reference-pulses method* on the amplitude of the pulse. As shown in Fig. 6, the reference-pulses of neutrons of three pulse height bins were obtained by averaging the neutron pulses in each bin respectively and the  $\gamma$ -ray reference-pulse was computed by averaging a total of 1103  $\gamma$ -ray pulses. The acquired average neutron and  $\gamma$ -ray pulses were used as references for identifying and distinguishing neutrons from  $\gamma$  rays measured with the

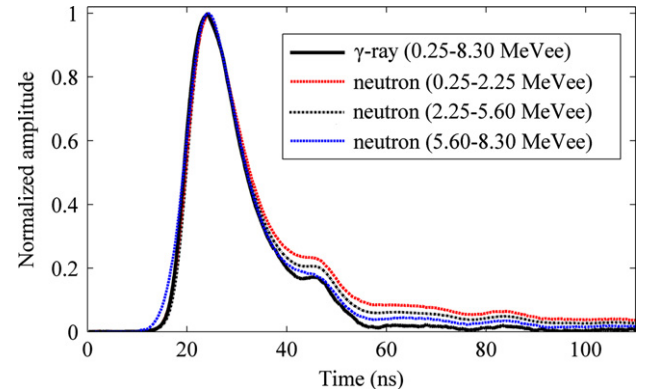


**Fig. 6.** The reference-pulses of neutrons in three pulse height bins and  $\gamma$  rays.

BC501A scintillator. Each measured pulse in some pulse height bin, after normalization, was compared point-by-point to the neutron reference-pulse of its bin and the  $\gamma$ -ray reference-pulse. The comparison of the pulse shapes was done from the pulse maximum to 110 ns after the pulse maximum; this is the optimized region that correctly identified most pulses.

Like the *power spectrum PSD method*, we use the Chi Square ( $\chi^2$ ) to evaluate the differences between the measured pulse and the reference-pulses of neutron and  $\gamma$  rays as follows:

$$\chi_{n,R}^2 = \sum_i \frac{(x_i - R_{n,i})^2}{R_{n,i}}, \chi_{\gamma,R}^2 = \sum_i \frac{(x_i - R_{\gamma,i})^2}{R_{\gamma,i}} \quad (7)$$

where  $x_i$  is the  $i$ -th sample of the pulse shape of the measured event,  $R_{n-i}$  and  $R_{\gamma-i}$  are the  $i$ -th samples of the reference-pulse shape of neutron and  $\gamma$ -ray events, respectively [22]. Then the  $n/\gamma$  discrimination parameter of this method is defined as:

$$D_R = \chi_{\gamma,R}^2 - \chi_{n,R}^2 \quad (8)$$

By plotting the peak amplitude of each measured pulse against the discrimination parameter  $D_R$  shown in Figs. 3–5b, two distinct groups of events can be observed in each plot. Similarly, each event has been denoted by a symbol corresponding to its TOF assignment and the threshold for discrimination has been depicted by a line. It is understandable that the region on the right of the discrimination line corresponds to neutrons and the left area corresponds to  $\gamma$  rays based on the *reference-pulses method*.

### 3.3. Performance comparison between the power spectrum PSD method and the reference-pulses method

Based on the discrimination rules of the *reference-pulses method* and the *power spectrum PSD method* described in Sections 3.1 and 3.2, the  $n/\gamma$  discrimination results of the three pulse height bins corresponding to different signal energies are derived from Figs. 3–5 and presented in Table 1.

$N_n$  and  $N_\gamma$  represent the number of the neutron and  $\gamma$ -ray pulses that incorrectly identified by the *reference-pulses method* or the *power spectrum PSD method* respectively.  $N_t$  is the total number of pulses in each bin. Thus the discrimination error of the *reference-pulses method* and the *power spectrum PSD method* can be calculated as

$$\text{Error} = (N_n + N_\gamma) / N_t \quad (9)$$

As shown in Table 1, the discrimination error of both the *reference-pulses method* and the *power spectrum PSD method* increase with the descending signal energies. However, the discrimination error of the *power spectrum PSD method* is lower than

**Table 1**  
Neutron/gamma discrimination results of the *reference-pulses* and the *power spectrum PSD methods* for different signal energies.

Energy (MeVee)	Method	$N_n$	$N_\gamma$	$N_t$	Error (%)
0.25–2.25	<i>The reference-pulses</i>	78	23	1714	5.9
	<i>The power spectrum</i>	48	17	1714	3.8
2.25–5.60	<i>The reference-pulses</i>	29	11	820	4.9
	<i>The power spectrum</i>	17	7	820	2.9
5.60–8.30	<i>The reference-pulses</i>	20	13	873	3.8
	<i>The power spectrum</i>	10	6	873	1.8

that of the *reference-pulses method* at different signal energies. Specifically, the discrimination error of the *power spectrum PSD method* is only 64.4, 59.2, and 47.4 percent of that of the *reference-pulses method* at the pulse height bins of 0.25–2.25 MeVee, 2.25–5.60 MeVee, and 5.60–8.30 MeVee, respectively. It is evident that the *power spectrum PSD method* shows increased discrimination accuracy over the *reference-pulses method*, especially at high particle energies.

In order to further evaluate the overall  $n/\gamma$  separation performance of the *power spectrum PSD method* and the *reference-pulses method*, the Figure of Merit (FOM) of the two methods will be obtained and compared with each other. A larger value of FOM indicates better performance of the  $n/\gamma$  discrimination method. FOM is a common measure of the separation that can be achieved between different types of event distributions and is defined as

$$\text{FOM} = \frac{S}{\text{FWHM}_\gamma + \text{FWHM}_n} \quad (10)$$

where  $S$  is the separation between the peaks of the neutron and  $\gamma$ -ray events in the spectrum,  $\text{FWHM}_n$  is the full-width-half-maximum (FWHM) of the spread of events classified as neutrons and  $\text{FWHM}_\gamma$  is the FWHM of the spread in the  $\gamma$ -ray peak. If the distribution function of each event is consistent with Gaussian distribution, Eq. (9) becomes

$$\text{FOM} = \frac{|\mu_n - \mu_\gamma|}{2.35(\sigma_\gamma + \sigma_n)} \quad (11)$$

where  $\mu_\gamma$  and  $\mu_n$  are the means of the  $\gamma$ -ray and neutron Gaussians respectively. The standard deviation,  $\sigma$ , is given as  $\sigma_\gamma$  and  $\sigma_n$  for the  $\gamma$ -ray and neutron Gaussians respectively [25].

To evaluate the separation of the neutron and  $\gamma$ -ray plumes in Fig. 4 for example, those data should be firstly normalized to the total number of pulses in bin 2 and then presented as a probability distribution function which has plotted against the distance of each point from the discrimination line (Fig. 7).

As shown in Fig. 7, two peaks of the distribution curve evidently correspond to the  $\gamma$ -ray and neutron events and can be used for Gaussian fits with the curve fitting tool available in MATLAB software. The sum of Gaussian distribution is expressed as

$$f(x) = A_\gamma \exp\left[-\frac{(x-\mu_\gamma)^2}{2\sigma_\gamma^2}\right] + A_n \exp\left[-\frac{(x-\mu_n)^2}{2\sigma_n^2}\right] \quad (12)$$

where  $\mu_\gamma$ ,  $\mu_n$ ,  $\sigma_\gamma$  and  $\sigma_n$  are the same as those in Eq. (11). The Gaussian functions are scaled using  $A_\gamma$  for the  $\gamma$ -ray Gaussian and  $A_n$  for the neutron Gaussian. It is obvious that there is a good fit between the Gaussian distribution and the probability distribution function. Table 2 presents the means, standard deviations with uncertainties for the Gaussian fits shown in Fig. 7.

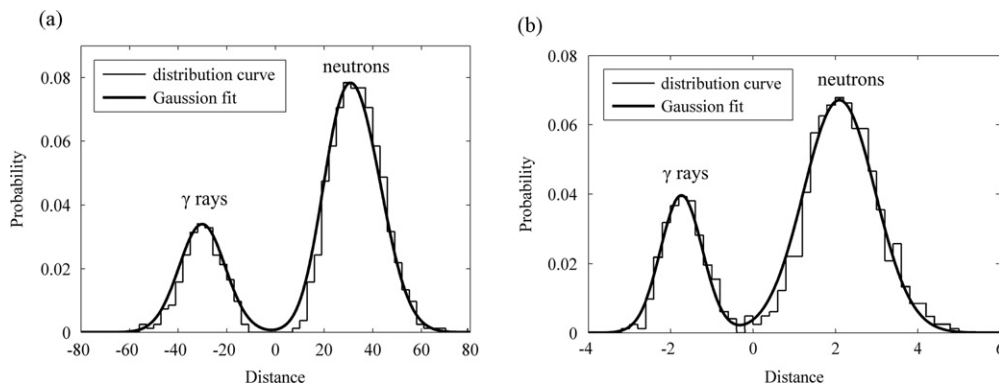


**Fig. 7.** The probability distribution histogram corresponding to Fig. 4 for pulses in bin 2 with fitted Gaussian distributions. (a) *The power spectrum PSD method*, and (b) *the reference-pulses method*.

**Table 2**

The values of parameters in (12) calculated from the experimental results of the *reference-pulses* and the *power spectrum PSD methods* for pulses in bin 2, respectively.

Method	$\mu_\gamma$	$\sigma_\gamma$	$\mu_n$	$\sigma_n$
<i>The reference-pulses</i>	$-1.742 \pm 0.001$	$0.615 \pm 0.001$	$2.091 \pm 0.002$	$0.784 \pm 0.001$
<i>The power spectrum</i>	$-30.156 \pm 0.169$	$9.472 \pm 0.053$	$30.783 \pm 0.172$	$9.586 \pm 0.058$

**Table 3**

FOMs of the reference-pulses and the power spectrum PSD methods for different signal energies.

Energy (MeVee)	FOM	
	<i>The reference-pulses</i>	<i>The power spectrum</i>
0.25–2.25	$1.005 \pm 0.001$	$1.024 \pm 0.001$
2.25–5.60	$1.166 \pm 0.001$	$1.360 \pm 0.002$
5.60–8.30	$1.421 \pm 0.002$	$1.614 \pm 0.002$

Substituting the variables in Eq. (11) with the corresponding data shown in Table 2, we can obtain the FOMs of the *reference-pulses* and the *power spectrum PSD methods* for bin 2 (2.25–5.60 MeVee). Similarly, the FOMs corresponding to different signal energies using both the *reference-pulses* and the *power spectrum PSD methods* have been calculated and listed in Table 3.

According to Table 3, the FOM of the *power spectrum PSD method* (FOM<sub>P</sub>) is approximately 16.6% and 13.6% larger than that of the *reference-pulses method* (FOM<sub>R</sub>) for bin 2 (2.25–5.60 MeVee) and bin 3 (5.60–8.30 MeVee) respectively, which indicates an evident improvement of the performance over the *reference-pulses method* under the same condition. However, FOM<sub>P</sub> is only 1.9% larger than FOM<sub>R</sub> for bin 1 (0.25–2.25 MeVee), which shows that the performance of these two PSD methods are comparable to each other when discriminating those neutrons at relatively low energies from  $\gamma$  rays.

#### 4. Summary and conclusions

In this paper, a novel  $n/\gamma$  discrimination method which makes use of the power spectrum of the signal from a BC501A liquid scintillator was presented. This *power spectrum PSD method* and the *reference-pulses method* were applied to the same signals acquired with the system comprising of a 14.1 MeV neutron generator, a BC501A liquid scintillator and a 5GSample/s 8-bit oscilloscope to discriminate neutrons and  $\gamma$  rays respectively. The performance of the *power spectrum PSD method* in terms of  $n/\gamma$  discrimination was evaluated and compared with that of the *reference-pulses method* for three pulse height bins (0.25–2.25 MeVee, 2.25–5.60 MeVee, and 5.60–8.30 MeVee).

The results demonstrated that the *power spectrum PSD method* gave considerable improvement over the *reference-pulses method* at relatively high energies because an improvement of 16.6% and 13.6% in FOM was observed for bin 2 (2.25–5.60 MeVee) and bin 3 (5.60–8.30 MeVee) respectively and its error rate of  $n/\gamma$  discrimination was lower than that of the *reference-pulses method*. This is because that some noise in the signal has the similar time-domain features with the particle signal which will directly change the pulse shape of the particle signal and as a result, those PSD methods which use time-domain features of the particle signals, e.g. the *reference-pulses method*, are sensitive to noise and statistical fluctuation of the light intensity. Therefore, it is noteworthy that a new definition of the discrimination parameter for the *reference-pulses method* was given in [15], which can cancel out part of the high frequency noise present in the signal and thus decrease this method's sensitivity to noise. However, the *power*

*spectrum PSD method* we proposed here is an essentially frequency-domain method, for the power spectrum of the particle signal is utilized to accomplish  $n/\gamma$  discrimination, and thus it outperforms the *reference-pulses method*. And this method is suited for the applications which use scintillator detectors and require PSD such as biomedical imaging, home-land security, worker safety and nuclear non-proliferation. Yet at the same time, it should be pointed out that the  $n/\gamma$  discrimination efficiency of the *power spectrum PSD method* is worsened for small signals due to the scintillation statistics, the electronic noise and the quantization effects of the digitizer, which is a fundamental limitation for any discrimination method and will be the subject of our future research.

#### Acknowledgments

This project was funded by the National Natural Science Foundation of China. We would like to acknowledge the support of the Institute of Nuclear Physics and Chemistry, the Chinese Academy of Engineering Physics, Mianyang, China. We also appreciate the help and advice of Dr. Li An and Dr. Pu Zheng and the technical team at the Chinese Academy of Engineering Physics, Mianyang, China.

#### References

- [1] G.F. Knoll, Radiation Detection and Measurement, third ed., Wiley, New York, 2000.
- [2] T.K. Alexander, F.S. Goulding, Nuclear Instruments and Methods in Physics Research 13 (1961) 244.
- [3] M. Roush, M.A. Wilson, W.F. Hornyak, Nuclear Instruments and Methods in Physics Research 31 (1964) 112.
- [4] F.D. Brooks, Nuclear Instruments and Methods in Physics Research 4 (1959) 151.
- [5] J.M. Adams, G. White, Nuclear Instruments and Methods in Physics Research 156 (1978) 459.
- [6] G. Ranucci, Nuclear Instruments and Methods in Physics Research Section A 354 (1995) 389.
- [7] M. Moszynski, G. Bizard, G.J. Costa, D. Durand, et al., Nuclear Instruments and Methods in Physics Research Section A 638 (2011) 116.
- [8] S.D. Ambers, M. Flaska, S.A. Pozzi, Nuclear Instruments and Methods in Physics Research Section A 638 (2011) 116.
- [9] S. Marrone, D. Cano-Ott, N. Colonna, C. Domingo, F. Gramegna, E.M. Gonzalez, F. Gunsing, M. Heil, F. Kappeler, P.F. Mastinu, et al., Nuclear Instruments and Methods in Physics Research Section A 490 (2002) 299.
- [10] N.V. Kornilov, V.A. Khriatchkov, M. Dunaev, A.B. Kagalenko, N.N. Semenova, V.G. Demenkov, A.J.M. Plompen, Nuclear Instruments and Methods in Physics Research Section A 497 (2003) 467.
- [11] B.D. Mellow, M.D. Aspinall, R.O. Mackin, M.J. Joyce, A.J. Peyton, Nuclear Instruments and Methods in Physics Research Section A 578 (2007) 191.
- [12] M.D. Aspinall, B.D. Mellow, R.O. Mackin, M.J. Joyce, N.P. Hawkes, D.J. Thomas, Z. Jarrah, A.J. Peyton, P.J. Nolan, A.J. Boston, Nuclear Instruments and Methods in Physics Research Section A 583 (2007) 432.
- [13] M.J. Joyce, M.D. Aspinall, F.D. Cave, K. Georgopoulos, Z. Jarrah, IEEE Transactions on Nuclear Science NS-57 (2010) 2625.
- [14] G. Liu, M.D. Aspinall, X. Ma, M.J. Joyce, Nuclear Instruments and Methods in Physics Research Section A 607 (2009) 620.
- [15] D. Savran, B. Lohrer, M. Miklavc, M. Vencelj, Nuclear Instruments and Methods in Physics Research Section A 624 (2010) 675.
- [16] S. Yousefi, L. Lucchese, M.D. Aspinall, Nuclear Instruments and Methods in Physics Research Section A 598 (2007) 551.
- [17] D.I. Shippen, M.J. Joyce, M.D. Aspinall, IEEE Transactions on Nuclear Science NS-57 (2010) 2617.
- [18] G. Liu, M.J. Joyce, X. Ma, M.D. Aspinall, IEEE Transactions on Nuclear Science NS-57 (2010) 1682.

- [19] J. Yang, X.L. Luo, G. Liu, C.B. Lin, Y.L. Wang, Q.Q. Hu, J.X. Peng, Chinese Physics C 36 (2012) 544.
- [20] S. Engelberg, Digital signal processing, An Experimental Approach, Springer, Berlin, 2008.
- [21] G.W. Corder, D.I. Foreman, Nonparametric Statistics for Non-Statisticians: A Step-by-Step Approach, Wiley, New York, 2009.
- [22] K.A.A. Gamage, M.J. Joyce, N.P. Hawkes, Nuclear Instruments and Methods in Physics Research Section A 642 (2011) 78.
- [23] M.D. Aspinall, Real Time Digital Assay of Mixed Radiation Fields, Ph.D. Dissertation, Lancaster Univ., Lancaster, 2007.
- [24] C. Guerrero, D. Cano-Ott, M. Fernández-Ordñez, E. González-Romero, T. Martínez, D. Villamarín, Nuclear Instruments and Methods in Physics Research Section A 597 (2008) 212.
- [25] R.A. Winyard, J.E. Lukin, B.W. McBeth, Nuclear Instruments and Methods in Physics Research 95 (1971) 141.